The first Italian micro exposure tool for EUV lithography: design guidelines and experimental results

F. Flora, S. Bollanti, P. Di Lazzaro, L. Mezi, D. Murra, and A. Torre

ENEA Frascati, Via E. Fermi 45, 00044 Frascati (Rome), Italy, flora@frascati.enea.it

ABSTRACT

The first Italian Micro Exposure Tool (MET) for EUV lithography has been developed at the ENEA Research Laboratories in Frascati. This tool (named MET-EGERIA) is based on a laser-plasma EUV source (named EGERIA), a couple of twin grazing-incidence collectors and a non-conventional Schwarzschild optics. In spite of the very low cost of the Schwarzschild optics, the specific design of the low vibration board and the innovative alignment technique (a modified Foucault technique) applied to the Schwarzschild optics allowed the achievement of a resolution better than 100 nm on a wafer coated with a PMMA photoresist.

The MET-EGERIA is also suitable for the coloration of lithium fluoride to be used in photonics, and is also a promising tool for nanobiotechnological research.

Keywords: laser-plasma, EUV lithography, Schwarzschild, exposure-tool

1 INTRODUCTION

Extreme UltraViolet (EUV) lithography represents the most promising technology for the next future of nano-electronics [1-3] as it is expected to support the Moore's law along the shrinking rate of electronic devices up to the 11nm half-pitch node.

The first Italian Micro Exposure Tool (MET) for EUV lithography has been developed at the ENEA Research Laboratories in Frascati [4]. As shown in Fig. 1, this tool (named MET-EGERIA) is based on a laser-plasma EUV source (named EGERIA), a couple of twin grazing-incidence collectors and a non-conventional Schwarzschild optics (SO).

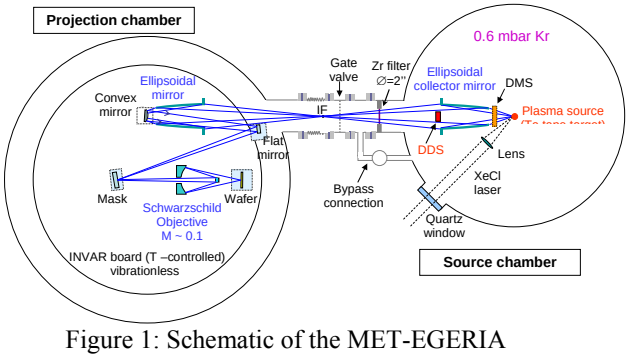

Figure 1: Schematic of the MET-EGERIA

A new type (patented) debris mitigation system (DMS) [5], based on krypton gas, reduces by three orders of magnitude the debris bombardment on the first collector. The use of Kr as a buffer gas forces the shift of the operating wavelength from the standard 13.5nm to 14.4 nm, since for shorter wavelengths the Kr transmission is too poor, as shown in Fig. 2. The high cross section of the interaction between Kr atoms with the plasma debris [6] allows to achieve with this gas a much better debris mitigation factor than with other gases.

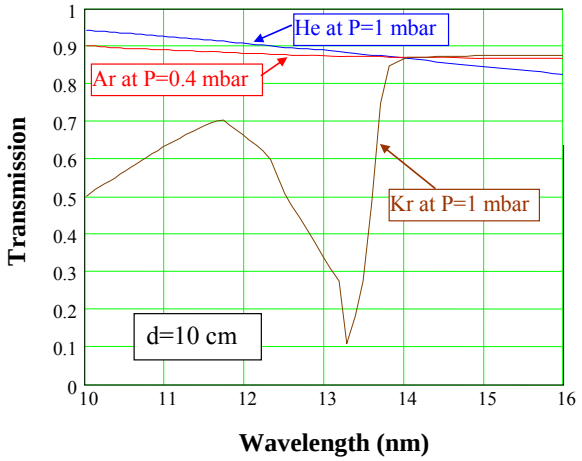

Figure 2: Transmission of Kr and other gases in the EUV over a length of 10 cm.

Hence, our DMS consists of the combination of a static low-pressure rare gas (typically Kr at ~1 mbar) with a mechanical device (typically a fan rotating at 6000 rpm). The gas slows down and stops the atomic component and the small particles, while the mechanical device halts the large/slow debris.

The ENEA DMS has been extensively tested and characterised in order to quantify its performances [7].

We measured the debris mitigation factors DMF ~ 450 for atoms and nanometric clusters, and DMF ~ 700 for particles larger than 500 nm, both emitted by a Cu plasma at a laser intensity in the 10^{10} W/cm^2 range. These DMF values, which for the particulate debris is at the forefront in this field, have been measured both through optical density measurements of the Cu layer deposited on glass plates and through the measurement of EUV-mirrors reflectivity degradation (both placed at the collector entrance). Fig. 3 shows one of these DMS efficiency tests, where the Ar and

Kr gas effect is compared (with the fan turning at 6000 r.p.m.). In the comparison, the Ar and Kr gas pressure values are chosen to give the same transmission at 14 nm (see Fig. 2).

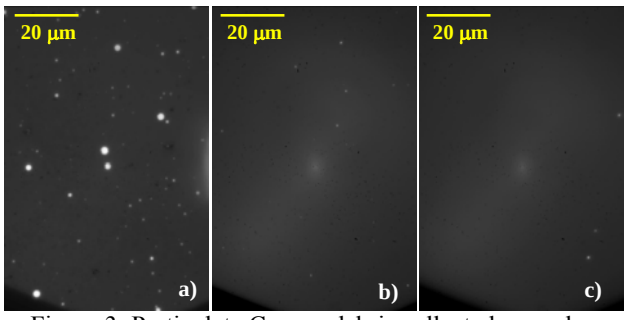

Figure 3: Particulate Copper debris collected on a glass plate at the first collector entrance after: 3 kshots in vacuum (a), 50 kshots in Ar gas at 0.4 mbar (b), 50 kshots in 1 mbar Kr gas (c).

The particular geometry of the collector (twin) yields to an almost isotropic illumination of the Schwarzschild optics, while the effects of the large (10°) mask tilt is compensated by a proper tilt of the wafer (see Fig. 1). Consequently an almost symmetric projection field of 300x300 μm^2 is achieved on the wafer plane.

2 ALIGNMENT OF THE SCHWARZSCHILD OPTIC

The SO consists of a convex and a concave holed spherical ML mirrors, put in concentric configuration (see Fig. 1 or 4). This optical system is much cheaper and relatively more simple to be aligned compared with other projection systems used for EUVL. Its drawback is the limited field of view, but it allows a very good geometrical resolution (comparable to or less than the diffraction limit) in a region close to the optical axis [8]. We improved the performances of a conventional SO by designing a modified configuration [9] that allows to keep the perfect concentricity of the mirrors even at large numerical aperture values, and recovering the worsening in resolution induced by the 10°-tilt of the mask with respect to the optical axis through a symmetrical, suitably scaled tilt of the wafer [10, 11]. The image field with resolution < 100 nm has in our case a linear dimension of ~ 300 µm.

Our SO mirrors have been made by Société Européenne de Systèmes Optiques, France. The SO has a numerical aperture NA = 0.23 and a magnification M ~ 1/10, which fixes at 27 nm its geometrical resolution limit for ideal spherical mirrors and a source on-axis. Combining this value with the 38-nm diffraction limit at λ = 14.4 nm, the best attainable theoretical resolution is 47 nm, which might be significantly increased due to a ≤ 8-nm SO global figure error. An accurate alignment of the two mirrors must be performed to approach its best performances, being the ~ 1-µm-tolerance spatial overlapping of the two curvature centers the most critical issue. Our SO holder is a single piece aluminum alloy cylinder with special thinned sections which allows three degrees of freedom: two of them are rotations of the concave mirror around two mutually orthogonal axes, both orthogonal to the optical axis, crossing each other at the mirror vertex, controlled by piezoelectric transducers. They allow ~ 2 µrad angular resolution, i.e. ≤ 0.3 µm spatial transverse resolution on the curvature-center sphere. The third degree of freedom is the translation of the convex mirror along the optical axis, controlled by means of an actuator with ~ 1 µm longitudinal resolution.

We exploited the well known Foucault technique [12], [13] to perform the SO alignment. The Foucault test consists of a knife edge cutting part of the beam near the focus of the SO to produce a shadow pattern, called foucaultgram, on a screen put behind the focal plane as shown in Fig. 4. The shape of a foucaultgram depends on the longitudinal position of the knife, as well as on the percentage of beam stopped. Most important, each type of aberration has a distinctive foucaultgram, which corresponds to the lateral displacement of the aberrated rays.

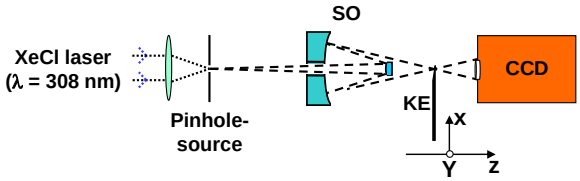

Figure 4: Schematic of the experimental set-up for the Foucault diagrams acquisition

Then, foucaultgrams allow to identify spherical and/or coma aberrations affecting the beam, and their relative weight. In principle, real-time alignment can be carried out with the observation and interpretation of these shadow patterns. The alignment method is an iterative process: when an aberration is identified, it is corrected until another aberration term becomes dominant. However, it is not a simple process: the experimental foucaultgram should be compared with a virtually infinite number of labelled foucaultgrams. In practice, even choosing the foucaultgram more similar to the experimental one, it is difficult to achieve quantitative information on the SO misalignment. As a consequence, the Foucault knife-edge test is mainly used for a qualitative estimation of optical systems misalignment.

In our case the in-band EUV power incident on the wafer was unexpectedly too low to perform an at-wavelength alignment in a reasonable time, so that we performed the Foucault test using ultraviolet light with a novel approach for overcoming the limitations related to the diffraction limit of the alignment wavelength.

In our set-up, an ultraviolet laser beam is focused on a pinhole to illuminate it with the central, quite uniform portion of the Airy disk, generating the point-like object-source of the SO (see Fig. 4). The SO image is cut at about its half by the knife edge (KE) near the focal plane of the SO, while the CCD camera (PI-MTE, Princeton Instrument) catches the corresponding foucaultgram.

The correct x-position of the KE is recognised when the transmitted power is half of the full power (without KE) for any longitudinal position of the KE. Then, a longitudinal scan of the KE allows to identify the SO aberration type and to evaluate its amount, in particular the spherical aberration induced by the longitudinal decentering of the mirrors curvature centres, and the coma aberration induced by their transverse non-overlapping of the mirrors centres. The first one is controlled by the longitudinal translation of the convex mirror, the second by the tilts of the concave one.

Figure 5 shows a sequence of measured foucaultgrams in presence of a significant spherical aberration. Beside the experimental foucaultgrams (first row), a sequence of foucaultgrams simulated by 2-D ray tracing with simple binary images and with an artificial diffraction effect are also reported in the 2nd and 3rd row of the figure, respectively. The binary foucaultgrams are obtained by addressing white color to all the pixels reached by at least one ray of the ray-tracing, while the diffracted-foucaultgrams on the 3rd row are obtained, for each z value, by averaging many binary foucaultgrams obtained for different beams whose foci are spread along x and y within the Airy disk (that is, within the diffraction limit area) of the beam used for the experimental foucaultgrams. In our case we used a 308 nm radiation and the corresponding Airy disk diameter at the focal plane is 2 μm. In practice, the spreading of the focal position of the different beams is equivalent to a knife shift along the X direction (still within the Airy disk diameter). The sequence of images in figure 5 shows that as the knife crosses the focal plane (z = 0) the shadow of the knife over half the beam on the CCD changes from right to left hand. The three radial shadows correspond to the spider mount holding the convex mirror (these shadows are artificially added also on the ray-tracing focaultgrams). When spherical aberration is present, the focus of the marginal (external) rays differs from that of the paraxial (internal) rays; consequently, when the knife is between the two extreme foci, the shadow for the paraxial rays (for example) moves to the left hand when that for the marginal rays is still on the right hand, so that a "double-C" structure appears on the foucaultgram.

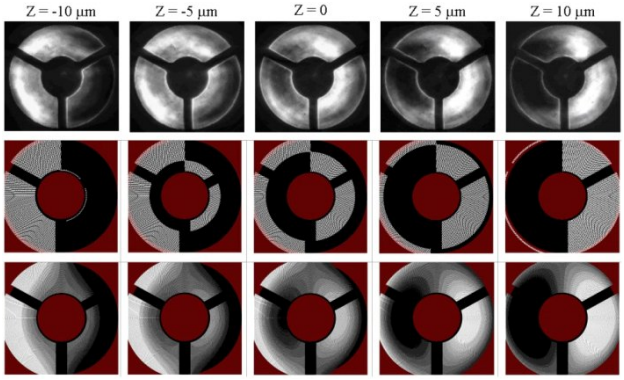

Figure 5. First row: Experimental sequence of foucaultgrams in presence of significant spherical aberration. The KE covers half the beam. The sequence was obtained by scanning the KE along the optical axis z. The z values are the KE positions referred to the middle point between the paraxial and marginal focus. Second row: 2-D ray tracing simulation of the same sequence obtained by shifting the concave mirror by 0.8 mm away from the concentric condition. Third row: the same 2-D ray tracing with artificial diffraction effect.

This effect is very clear in the second row of figure 5 where no diffraction is present. When dealing with an ideal geometrical beam without diffraction it would be very easy to estimate the z-position of the two extreme foci from the experimental foucaultgrams sequence (just by finding the two z-positions of the knife where the "double-C" structure disappears), that is the amplitude of the longitudinal spherical aberration. This is obviously true for every kind of aberrations. Unfortunately real beams suffer of diffraction, and as a consequence the estimation of small aberration amplitude becomes more difficult or even impossible. For this reason the possibility to simulate the foucaultgrams sequences with artificial diffraction effects (that is changing the alignment parameters in the 2-D ray tracing until the best agreement between experimental and simulated sequences is reached) is helpful to estimate the SO aberration amplitude and to properly correct the SO alignment parameters.

Since the diffraction effects of the UV wavelength conceal the aberration diagrams as the alignment improves, in order to find the values of the three SO adjusting parameters which vanish the aberrations we repeatedly induced quantifiable aberration amounts through controlled misalignments, finding the relations between them, and finally deducing the best alignment values by interpolation.

3 RESULTS

The exposures were performed using a mask with Cr absorbing grating with variable period, starting from 8-µm down to 1-µm half-pitch line-space. The used resist was 996,000-Molecular Weight, 100-nm thick polymethyl-methacrylate (PMMA) spin-coated on Si wafer. It was exposed to a total fluence of ~ 10 mJ/cm^2, then developed and observed at the Atomic Force Microscope (AFM). Figure 6 shows the 2-D image of the patterned PMMA in the region corresponding to the 160 nm half-pitch line-space pattern.

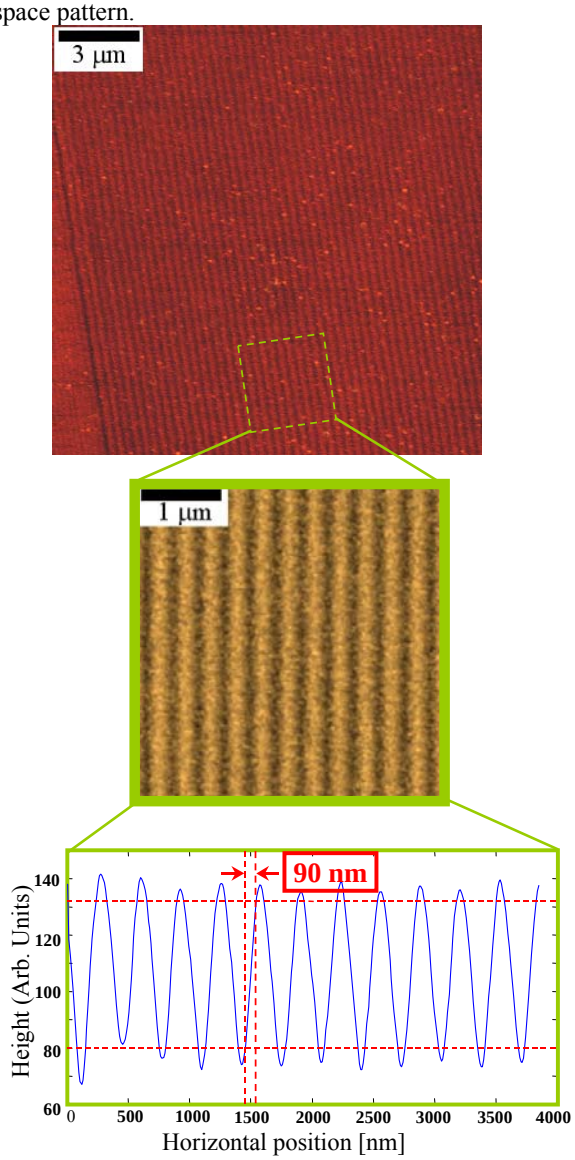

Figure 6: 160 nm half.pitch lines obtained on a PMMA photoresist with the MET-EGERIA tool

On these lines we measured the highest resolution, taken as the distance required for the edge response to rise from 10% to 90%. Notwithstanding the patterns is not at a full resist height, probably due to a still insufficient fluence for the used resist, the obtained resolution is 90 nm.

4 CONCLUSIONS

We have presented characteristics and performance of a micro-exposure tool for projection lithography at 14.4 nm developed at the ENEA Research Centre in Frascati within a National Project on nanotechnologies,. The huge emission of fast atoms and particulate from the laser-produced-plasma is strongly attenuated by a patented debris mitigation system (DMS), in order to preserve the expensive elliptical mirror that acts as collector. Mitigation factors up to 450 and 700 have been obtained for atoms and particles, respectively, which are at the fore-front of this matter.

The cleaned radiation pulses are properly shaped by the illumination optics up to the mask reflecting the patterns to be reproduced. The projection optics is a low-cost suitably designed Schwarzschild objective (SO), whose alignment has been carried out by the Foucault technique using ultraviolet light. We used a novel procedure to overcome the limitations related to the diffraction limit of the alignment wavelength.

We achieved 90-nm-resolution patterning (taken as the distance required for the edge response to rise from 10% to 90%) on PMMA resist by our laboratory-scale tool based on a Schwarzschild-type projection optics.

The modulation amplitude of these 160 nm half pitch lines was as large as 80% of that of wider lines (up to those with 0.8 µm half pitch). The obtained resolution is among the best ever achieved by low-cost, laboratory-scale EUVL METs.

REFERENCES

[1] J. Roberts et al., Microelectron. Eng., 83, 672, 2006.
[2] K. Kemp and S. Wurm , C.R. Phys., 7, 875, 2006.
[3] P. J. Silverman, J. Microlithogr. Microfabr. Microsyst., 4, 2005.
[4] S. Bollanti et. al., European Physics Letters, 84, 58003, 2008.
[5] European Patent number: EP1211918, see: http://v3.espacenet.com/textdoc?DB=EPODOC&IDX=EP1211918&F=0&QPN=EP1211918
[6] F. Flora et al. , Europhys. Lett., 56, 676, 2001.
[7] S. Bollanti at al., Proc. SPIE 6703, 670308, 2007.
[8] I. A. Artioukov and K. M. Krymski, Opt. Eng., 39, 2163, 2000.
[9] A. Budano et al., Appl. Opt., 45, 4254, 2006.
[10] S. Bollantiet al., Appl. Phys. B, 85, 603, 2006.
[11] S. Bollanti, et al., Appl. Phys. B, 91, 127, 2008.
[12] M. L. Foucault, C. R. Acad. Sci. Paris,47, 958 , 1858.
[13] R. B. Korsmeyer, Sky & Telescope, 3, 18, 1944.

[1] Flora Francesco, ENEA, Via E. Fermi 45, 00044 Frascati, (Rome), Italy, Ph: (+39) 06-94005745, Fax: (+39) 06-94005334, flora@frascati.enea.it